

Semantic Communication-Enabled Wireless Adaptive Panoramic Video Transmission

Haixiao Gao, Mengying Sun, Xiaodong Xu, Shujun Han
State Key Laboratory of Networking and Switching Technology
Beijing University of Posts and Telecommunications, Beijing, China
Email: {haixiao, smy_bupt, xuxiaodong, hanshujun}@bupt.edu.cn

Abstract—In this paper, we propose an adaptive panoramic video semantic transmission (APVST) network built on the deep joint source-channel coding (Deep JSCC) structure for the efficient end-to-end transmission of panoramic videos. The proposed APVST network can adaptively extract semantic features of panoramic frames and achieve semantic feature encoding. To achieve high spectral efficiency and save bandwidth, we propose a transmission rate control mechanism for the APVST via the entropy model and the latitude adaptive model. Besides, we take weighted-to-spherically-uniform peak signal-to-noise ratio (WS-PSNR) and weighted-to-spherically-uniform structural similarity (WS-SSIM) as distortion evaluation metrics, and propose the weight attention module to fuse the weights with the semantic features to achieve better quality of immersive experiences. Finally, we evaluate our proposed scheme on a panoramic video dataset containing 208 panoramic videos. The simulation results show that the APVST can save up to 20% and 50% on channel bandwidth cost compared with other semantic communication-based and traditional video transmission schemes.

Index Terms—Semantic communication, panoramic video, latitude adaptive, weight attention

I. INTRODUCTION

In the vision of 6G, immersive communication will be a key application scenario where users are invited to watch 360-degree panoramic videos and interact with the virtual world [1]. To ensure the quality of experience (QoE), it needs to provide low-latency and high-quality video transmission with less than 20 ms [2], [3]. However, for a 4K video (3840×1920), the user can actually view the image at a resolution of approximately 960×540 because of the limitations of field of view. Therefore, it needs to transmit high-resolution panoramic video to achieve a greater immersive experience, which leads to a dramatic increase in the amount of data transmitted.

Current panoramic video transmission schemes are designed based on the traditional wireless communication system, and these schemes employ bitrate selection, resource allocation, and other strategies to achieve low-latency and high transmission performance metrics [4]. However, traditional bit-level error-free transmission methods struggle to support the transmission of massive amounts of data, such as panoramic videos. As one of the key enabling technologies for 6G, semantic communication is taken into account to enhance the transmission efficiency [5]–[7]. Unlike traditional bit-oriented communication, it aims to pursue higher “semantic fidelity” rather than error-free transmission of symbols. By applying neural networks, artificial intelligence enables the extraction and recovery of

semantic features of information, thus reducing the amount of data transmitted and achieving semantic-level compression of image, text, speech, and other types of information [8], [9].

In order to achieve efficient transmission of video, there has been a lot of research on how to employ neural networks for video transmission. Li *et al.* build the deep contextual video compression (DCVC) network [10], which extracts rich high-dimensional contextual information by the correlation between frames to transmit videos. After that, Wang *et al.* of [11] proposed the deep video semantic transmission (DVST) network, which takes the semantic communication into account. The DVST network achieves semantic transmission of video by nonlinear transforms and deep joint source-channel coding (Deep JSCC) under the guidance of the entropy model. In this paper, to transmit the panoramic video, we first apply Equirectangular Projection (ERP) to project spherical video on a flat surface. However, due to the characteristics of the ERP [12], there would be a large information redundancy if panoramic videos are transmitted directly by the DCVC and DVST networks. At the same time, it will cause a decrease in the panoramic video evaluation metrics weighted-to-spherically-uniform peak signal-to-noise ratio (WS-PSNR) [13] and weighted-to-spherically-uniform structural similarity (WS-SSIM) [14] which mean the quality of immersive experience.

In order to improve the transmission efficiency of panoramic videos and bring better immersive QoE, a more efficient end-to-end communication system is needed. The contributions of this paper are summarized as follows: 1) We propose an end-to-end efficient adaptive panoramic video semantic transmission network, i.e., APVST. The proposed APVST is based on the Deep JSCC structure and attention mechanism to adaptively extract semantic features from panoramic frames and achieve variable-length encoding of semantic information. 2) To achieve higher WS-PSNR and WS-SSIM, we propose a weight attention (WA) module to learn the correlation between weights and semantic features for higher-quality panoramic video transmission. 3) Since ERP causes the information redundancy on different latitudes, we propose a latitude adaptive module which can reduce the bandwidth for panoramic video transmission by combining it with the entropy model.

II. THE PROPOSED APVST SCHEME

In this section, we introduce the overall transmission framework of APVST, WA module, and latitude adaptive module.

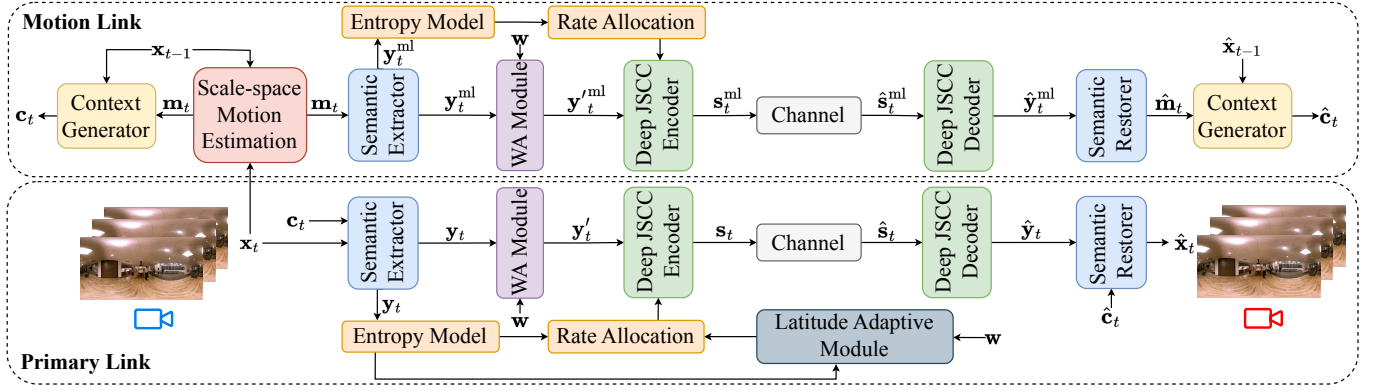


Fig. 1. The framework of APVST

Finally, the optimization process is designed.

A. The Framework of APVST

The proposed APVST framework is shown in Fig. 1, which consists of the motion link and the primary link. Referring to [10] [11], based on the rich correlation information between current and reference panoramic frames, the APVST estimates the motion information \mathbf{m}_t and transmits it to the receiver through the motion link. Based on the motion information and reference panoramic frame, the context generation network extracts the context \mathbf{c}_t and $\hat{\mathbf{c}}_t$, respectively. The primary link adaptively converts the source frames into potential representations in the semantic feature domain with the context. To enable wireless transmission, the semantic information is encoded at variable length by the Deep JSCC encoder, while the code rate is jointly guided by the learnable latitude adaptive module and entropy model. Due to the similarity between the primary link and the motion link, the transmission process of panoramic video on the primary link will be introduced in detail.

After the motion link generates \mathbf{c}_t and $\hat{\mathbf{c}}_t$, the primary link automatically learns the correlation between the current frame \mathbf{x}_t and \mathbf{c}_t to remove the information redundancy. The semantic feature map \mathbf{y}_t is extracted on the basis of \mathbf{c}_t and encoded into the corresponding codeword sequence \mathbf{s}_t by Deep JSCC encoding, i.e.,

$$\mathbf{y}_t = f_{SE}(\mathbf{x}_t|\mathbf{c}_t) \text{ and } \mathbf{s}_t = f_{JE}(\mathbf{y}'_t), \quad (1)$$

where f_{SE} and f_{JE} denote the function of the semantic extractor and Deep JSCC encoder in the primary link, respectively. As the input to the encoder, the weighted spatial attention feature \mathbf{y}'_t is obtained by the WA module. The symbols through wireless channel is $\hat{\mathbf{s}}_t = \mathbf{s}_t + \mathbf{n}_t$, where $\mathbf{n}_t \sim \mathcal{N}(0, \sigma^2 \mathbf{I}_{k_t})$ is the noise of primary link and k_t represents the dimension of \mathbf{s}_t . The recovered frames are reconstructed through Deep JSCC decoding and semantic recovery, which can be expressed as

$$\hat{\mathbf{y}}_t = f_{JD}(\hat{\mathbf{s}}_t) \text{ and } \hat{\mathbf{x}}_t = f_{SR}(\hat{\mathbf{y}}_t|\hat{\mathbf{c}}_t), \quad (2)$$

where f_{JD} and f_{SR} denote the function of semantic restorer and Deep JSCC decoder of primary link, respectively.

The APVST network is adept at autonomously learning the inter-frame correlations in panoramic videos, which is crucial for both semantic extraction and recovery. This network is particularly designed to consider key evaluation metrics during the transmission of panoramic frames, leveraging a weighted spatial attention map to significantly enhance the immersive experience, i.e., WS-PSNR and WS-SSIM. The encoding and decoding processes are meticulously guided by the entropy model and the latitude adaptive module. These components are instrumental in recognizing and adapting to the unique attributes of panoramic videos, thereby enabling targeted automatic encoding for specific regions. By this approach, APVST can effectively reduce information redundancy and achieve the efficient transmission of panoramic videos.

B. WA Module

To measure the quality of panoramic video in the observation space more accurately, the evaluation metrics WS-PSNR and WS-SSIM take into account the panoramic frames structure information [13], [14]. These metrics combine the distortion relationship between projection planes and user's field of view to map the spherical distortion to the 2D plane distortion, which can describe the immersive subjective experience quality more accurately in viewing panoramic video.

Inspired by the spatial attention module which is proposed in [15], to obtain higher WS-PSNR and WS-SSIM which mean the immersive experience of users, we combine initial weight map \mathbf{w} and feature map \mathbf{y}_t to achieve weighted spatial attention by the neural networks. The weighted spatial attention map \mathbf{M}_t in the primary link can be obtained as

$$\begin{aligned} \mathbf{M}_t &= \sigma(\text{Conv}_{3 \times 3}^2 \{ \text{AvgPool}^4(\mathbf{w}); \text{MaxPool}^4(\mathbf{w}); \mathbf{y}_t \}) \\ &= \sigma(\text{Conv}_{3 \times 3}^2 \{ \mathbf{F}_{\text{Avg}}; \mathbf{F}_{\text{Max}}; \mathbf{y}_t \}), \end{aligned} \quad (3)$$

where AvgPool^4 and MaxPool^4 denote that the initial weight maps $\mathbf{w} = \{w_{ij}\} \in \mathbb{R}^{H \times W}$ is downsampled by successive average pooling and maximum pooling four times. H and W represent the height and width of panoramic frames, respectively. Besides, a dimension is inserted into the pooling results to represent the number of channels, so the generated feature weight distributions are $\mathbf{F}_{\text{Avg}} \in \mathbb{R}^{1 \times \frac{H}{16} \times \frac{W}{16}}$

and $\mathbf{F}_{\text{Max}} \in \mathbb{R}^{1 \times \frac{H}{16} \times \frac{W}{16}}$, respectively. $\text{Conv}_{3 \times 3}^2$ denotes two successive convolution operations with convolution kernel of 3×3 , and σ is the Sigmoid activation function. Besides, the weight values decrease gradually from the equator to the poles and the distribution of w_{ij} is given as

$$w_{ij} = \cos \left(\left(i - \frac{H}{2} + \frac{1}{2} \right) \times \frac{\pi}{H} \right). \quad (4)$$

Similar to the primary link, the weighted spatial attention map \mathbf{M}_t^{ml} in motion link can be obtained as

$$\begin{aligned} \mathbf{M}_t^{\text{ml}} &= \sigma \left(\text{Conv}^{3 \times 3} \left\{ \text{AvgPool}^4(\mathbf{w}); \text{MaxPool}^4(\mathbf{w}); \mathbf{y}_t^{\text{ml}} \right\} \right) \\ &= \sigma \left(\text{Conv}^{3 \times 3} \left\{ \mathbf{F}_{\text{Avg}}; \mathbf{F}_{\text{Max}}; \mathbf{y}_t^{\text{ml}} \right\} \right). \end{aligned} \quad (5)$$

The feature information after deflation is obtained by multiplying the feature map with the points corresponding to the weighted spatial attention map. This process can be described as $\mathbf{y}_t^{\prime \text{ml}} = \mathbf{y}_t^{\text{ml}} \otimes \mathbf{M}_t^{\text{ml}}$ in the motion link and $\mathbf{y}_t' = \mathbf{y}_t \otimes \mathbf{M}_t$ in the primary link, respectively.

By utilizing the potent learning capabilities of neural networks, a correlation is established between weight maps and feature maps. Similar to the attention mechanism, this process assigns weights to each point on the feature map and enhances attention to regions with higher weight values during the information recovery phase. Consequently, such an approach leads the quality of the user's immersive experience WS-PSNR and WS-SSIM to be further improved.

C. Latitude Adaptive Module

Due to the characteristics of ERP, it stretches the pixels at different latitudes to different degrees. According to the work in [12], the higher latitude needs more pixels to represent it. In other words, it needs more bits to represent high-latitude pixels if a uniform compression strategy is used.

To reduce the information redundancy of transmission and improve the transmission efficiency of panoramic video, we propose the latitude adaptive network. For such a network, we design the adaptive weight feature map $\boldsymbol{\omega}_t = \{\omega_{t,mn}\} \in \mathbb{R}^{\frac{H}{16} \times \frac{W}{16}}$, which can be expressed as

$$\omega_{t,mn} = \eta_{t,mn} w_{mn}^{\text{AAP}} + 1 - \eta_{t,mn}, \quad (6)$$

where $\omega_{t,mn}$ denotes the adaptive weight feature value corresponding to the feature point (m, n) at moment t . w_{mn}^{AAP} denotes the weight value of \mathbf{w} after the adaptive average pooling (AAP) operation. $\eta_{t,mn}$ denotes the adaptive weight factor value of weight factor map $\boldsymbol{\eta}_t = \{\eta_{t,mn}\} \in \mathbb{R}^{\frac{H}{16} \times \frac{W}{16}}$, which is learned by the network according to the magnitude of entropy information. It can be expressed as $\boldsymbol{\eta}_t = f_{\text{AW}}(\mathbf{e}_t)$, where f_{AW} denotes the function of adaptive weight factor network and $\mathbf{e}_t = \{e_{t,mn}\} \in \mathbb{R}^{\frac{H}{16} \times \frac{W}{16}}$ means the entropy map corresponding to the feature map.

In order to achieve adaption of feature information dimension in latitude, the dimensions of the information in the wireless channel cannot exceed the limit of the maximum

dimension given in the corresponding latitude. This constraint can be expressed as

$$l_{t,mn} \leq \omega_{t,mn} \times \max(\mathcal{Q}), \quad (7)$$

where $l_{t,mn}$ denotes the information dimension corresponding to feature point (m, n) by quantizing, which can be expressed as the number of channels. $\max(\mathcal{Q})$ is the maximum value of the quantized set, which is given in Section IV. Therefore, the loss function of this module is expressed as

$$\mathcal{L}_t^{\text{la}} = \sum_m \sum_n \max(0, \omega_{t,mn} \times \max(\mathcal{Q}) - l_{t,mn}). \quad (8)$$

However, the quantization operation tends to cause gradient dispersion [16], we convert the dimensional restriction to the entropy restriction in the training phase, i.e.,

$$\mathcal{L}_t^{\prime \text{la}} = \sum_m \sum_n \max(0, \omega_{t,mn} \times \max(\mathbf{e}_t) - e_{t,mn}). \quad (9)$$

With the latitude adaptive module, the entropy model can more accurately compute the entropy of feature maps in different latitudes and achieve efficient transmission of panoramic videos.

D. Optimization Goal

The APVST network aims to maximize the transmission quality of frames with the minimum channel bandwidth overhead. In fact, the frames are transmitted continuously, N consecutive frames are one group of pictures (GoP). In the training phase, as shown in Fig. 1, the previously recovered panoramic frame is used as the reference frame for the current frame to achieve panoramic video transmission. Therefore, the loss function is formulated as follows:

$$\mathcal{L} = \frac{1}{N} \sum_{t=1}^N \left(D_t + \alpha \sum_m \sum_n (e_{t,mn} + e_{t,mn}^{\text{ml}}) + \beta \mathcal{L}_t^{\prime \text{la}} \right), \quad (10)$$

where D_t represents the magnitude of image distortion, which is chosen as the weighted mean squared error (WMSE) for WS-PSNR, and as the inverse of WS-SSIM for WS-SSIM to indicate the distortion of frames [13], [14]. To minimize channel bandwidth overhead, we take the entropy $e_{t,mn}$ in the primary link and $e_{t,mn}^{\text{ml}}$ in motion link into account, which can be expressed as the channel bandwidth cost. α and β denote the balance coefficients, which are constants.

III. INTERNAL STRUCTURE OF APVST

In this section, we introduce the internal structure of the APVST network. The disassembled parts of the internal structure are shown in Fig. 2 and Fig. 3. Since the structures of primary and motion links are similar, the primary link will be introduced in detail.

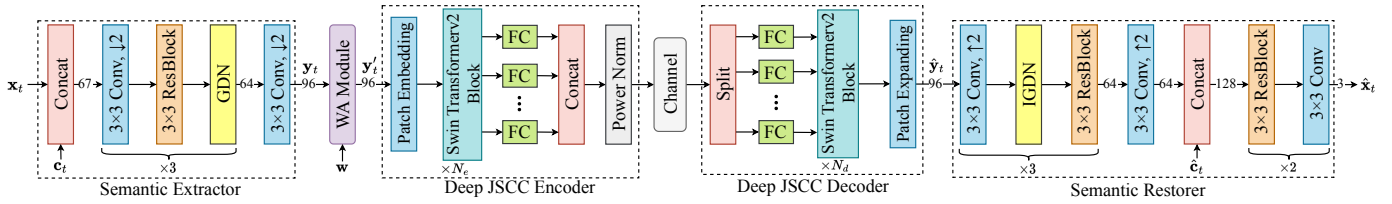


Fig. 2. Network architectures of the primary link. $k \times k$ Conv is a convolution with $k \times k$ filters, and the output channels of convolution are given on horizontal line. $\uparrow 2$ and $\downarrow 2$ indicate upsampling and downsampling with a stride of 2. GDN denotes the Generalised Divisive Normalization in [19], IGDN denotes the inverse operation of GDN.

A. The Overall Structure of APVST

As shown in Fig. 2, the overall structure of APVST includes semantic recovery and extraction as well as Deep JSCC encoding and decoding.

Referring to [10], the current panoramic frame \mathbf{x}_t is firstly concatenated with the context \mathbf{c}_t . Then, we achieve semantic extraction by successive downsampling convolutions, residual structure (Resblock), and GDN. In semantic recovery, as opposed to semantic extraction, the recovered feature map is upsampled successively by convolution with IGDN and Resblocks. Finally, we fuse $\hat{\mathbf{c}}_t$ with the upsampling result and adjust the number of channels by convolution layer and Resblocks.

In particular, the scale-space motion estimation in motion link refers to the scale-space flow, which is proposed in [17]. Compared to the traditional optical flow, it takes into account the scale space to generate scale parameters and act on the scale-space warp. Consequently, the network can achieve motion estimation efficiently when performing complex scenarios involving occlusion and rapid object movement.

The Deep JSCC structure employs symmetric encoding and decoding techniques. Drawing inspiration from [11], and to further augment the capacity of Deep JSCC in capturing long-term correlations, we integrate the swin transformer v2 as the backbone of both the Deep JSCC encoder and decoder, and take multi-head self-attention (MHSA) as the core of the network. In contrast to the original swin transformer, the swin transformer v2 utilizes cosine similarity and nonlinear relative position bias to enhance the network's robustness against various downstream tasks [18].

The Deep JSCC encoder is guided by the entropy model and the latitude adaptive module to achieve the variable-length encoding of the feature map. The information dimension $l_{t,mn}$ is derived by quantizing the entropy $e_{t,mn}$ into the set of quantized values, which can be expressed as $l_{t,mn} \in \mathcal{Q} = \{q_1, q_2, \dots, q_I\}$ with size I . The feature information dimension is adjusted by multiple learnable fully connected (FC) layers, and power normalization is performed before the information is transmitted into the channel.

B. The Structure of Enabling Modules

Fig. 3 shows in detail the structure of modules which are used to enhance the panoramic video transmission efficiency.

The context generation module generates context \mathbf{c}_t and $\hat{\mathbf{c}}_t$ based on motion information and reference panoramic frame.

This ensures that APVST can perform long-term learning and stable prediction. The structure of this network module is depicted in Fig. 3(a). Since the reference frame is subjected to convolution and Resblock, a scale-space warp operation is applied to capture the complex motion information. To address the issue of semantic information discontinuity caused by the warp operation and effectively generate the context, the warped result is further refined using Resblock and convolution.

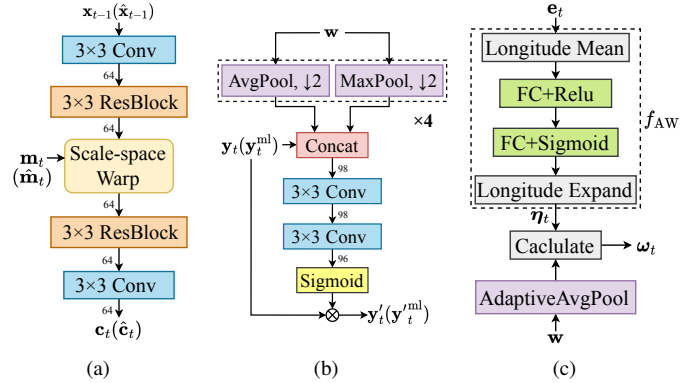


Fig. 3. Detailed structures of (a) Context Generator, (b) WA Module, and (c) Latitude Adaptive Module.

The proposed WA module deflates the feature maps appropriately to enhance the final video quality evaluation metrics, which structure is illustrated in Fig 3(b). To maximize the retention of weight map information, we combine the original weight map \mathbf{w} and the semantic feature map \mathbf{y}_t . Due to the different sizes of \mathbf{w} and \mathbf{y}_t , we employ two different pooling downsampling methods (four consecutive average pooling and maximum pooling) to act on \mathbf{w} . The obtained result is concatenated with \mathbf{y}_t , and the weighted spatial attention map \mathbf{M}_t is finally obtained by the Sigmoid activation function after two layers of convolution operation. The first convolution layer is designed to learn the relationship between \mathbf{M}_t and \mathbf{y}_t , while the second layer adjusts the number of channels.

The application of the latitude adaptive module enhances the transmission efficiency of panoramic videos. By utilizing function f_{AW} , the adaptive weight feature map ω_t is derived from entropy map $e_{t,mn}$ and original weight map \mathbf{w} . The detailed module structure is shown in Fig 3(c). Given that the semantic feature map information is more latitude-sensitive, a conversion from $\mathbf{e}_t \in \mathbb{R}^{\frac{H}{16} \times \frac{W}{16}}$ to $\mathbb{R}^{\frac{H}{16}}$ is performed by

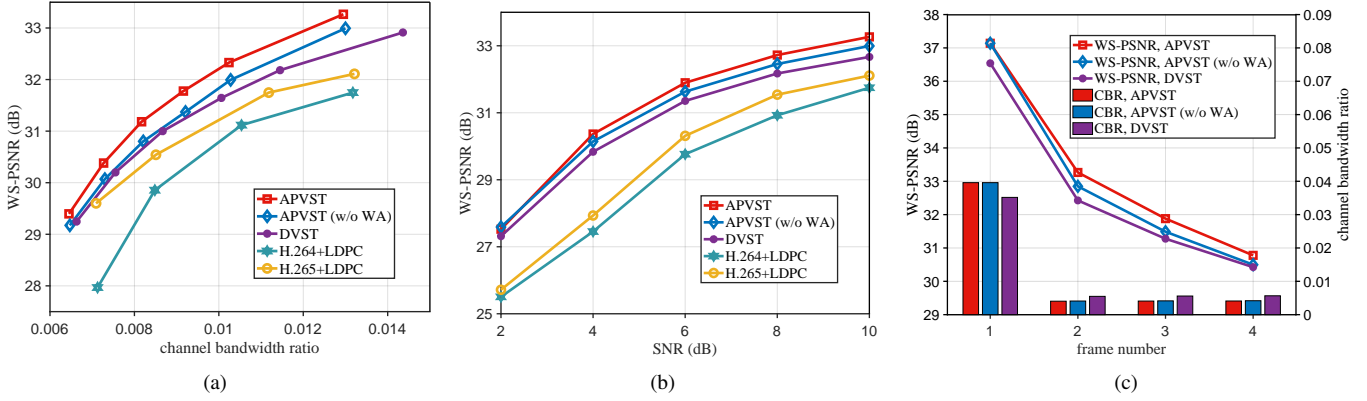


Fig. 4. (a) WS-PSNR performance versus channel bandwidth ratio (CBR), (b) WS-PSNR performance versus SNR, and (c) WS-PSNR and CBR in a GoP over the AWGN channel at SNR=10dB.

averaging over longitude. Subsequently, the weight factor map η_t is generated through FC layers using ReLU and Sigmoid activation functions and an expansion along the longitude is applied to transform $\mathbb{R}^{\frac{H}{16}}$ back to $\mathbb{R}^{\frac{H}{16} \times \frac{W}{16}}$. Finally, η_t and w are merged to compute ω_t according to equation (6).

IV. EXPERIMENTAL RESULTS

This section presents the training and testing datasets, details of parameter settings, and analysis of experimental results. By simulation analysis, we demonstrate the superiority of our proposed scheme compared with other video transmission schemes.

A. Experimental Environment

The proposed APVST is trained on the panoramic video dataset of 360VDS [20], the dataset of which contains 590 panoramic videos in ERP. The panoramic frames are resized to 512×256 pixels and randomly flipped during training. We evaluate the APVST on the VR scene dataset [21], which contains 208 panoramic videos. For the first frame (I-frame) coding of a GoP, we apply nonlinear transform source-channel coding (NTSCC) [22].

In this experiment, the number of blocks in swin transformerv2 is set to $N_e = N_d = 4$. 8 heads and 8×8 window size are used in MHSA. The quantization sets in Deep JSCC of the primary and motion links are set as $\mathcal{Q} = \{0, 2, 4, 6, 8, 10, 16, 20, 26, 32, 20, 48, 56, 64, 80, 96\}$ and $\mathcal{Q}^{ml} = \{0, 2, 4, 6, 8, 16, 32, 48\}$, respectively. The balance coefficients are set as $\alpha = 1/16$ and $\beta = 1/16$. In the model training and testing processes, we set the GoP sizes as $N = 7$ and $N = 4$, respectively. Adam optimizer is adopted as the optimizer. Other parameters are set as: learning rate is 10^{-4} , training batch size is 8, and testing batch size is 1. The whole APVST model was trained on a single A40 GPU for 4 days.

B. Analysis of Experimental Results

To validate the effectiveness of our proposed APVST scheme in terms of panoramic video transmission, we introduce four schemes for comparison. For semantic communication video transmission schemes, we consider “APVST (w/o WA)” and

“DVST” [11], where “APVST (w/o WA)” represents the APVST network without WA module. For traditional video transmission schemes, we consider “H.264 + LDPC” and “H.265 + LDPC”, which employ standard video codecs H.264 and H.265 for source coding and low-density parity check (LDPC) for channel coding. For RGB three-channel panoramic frames, we utilize the channel bandwidth ratio (CBR) [23] to indicate the average ratio of valid symbols transmitted in the channel within a GoP, where CBR can be expressed as $\frac{1}{N} \sum_{t=1}^N \frac{k_t}{H \times W \times 3}$ and k_t represents the dimension of s_t .

Fig. 4(a) shows WS-PSNR achieved by the five schemes varies with CBR. The test SNR is set as 10dB. Owing to the incorporation of the WA module and the latitude adaptive module, our proposed APVST can save approximately 20% and 10% on channel bandwidth cost compared with APVST (w/o WA) and DVST, respectively. Compared with H.264 + LDPC and H.265 + LDPC schemes, the proposed APVST can save bandwidth by about 50% and 40%, respectively. These results show the efficiency of our proposed APVST for panoramic video transmission. However, it can be observed that the WS-PSNR achieved by APVST (w/o WA) and DVST are quite similar at lower CBRs. This indicates that the entropy calculated under the guidance of the entropy model and the latitude adaptive network is smaller, and consequently, the impact of \mathcal{L}_t^{la} in Equation (9) is also reduced.

Fig. 4(b) shows WS-PSNR achieved by the five schemes varies with SNR. To ensure fairness, the same CBR is maintained for all schemes. At low SNR levels, semantic transmission significantly outperforms traditional video transmission schemes, which means that the proposed APVST has superior noise immunity properties. However, APVST and DVST achieve the same WS-PSNR at low SNR. This is attributed to the WA module, which primarily learns from the semantic feature map y_t and the weight map w during the training phase, without incorporating noise-related information, thereby reducing the noise immunity of the network.

Fig. 4(c) shows WS-PSNR and CBR achieved by the three semantic communication schemes vary with frame number within a GoP. Since the I-frame transmission is without a ref-

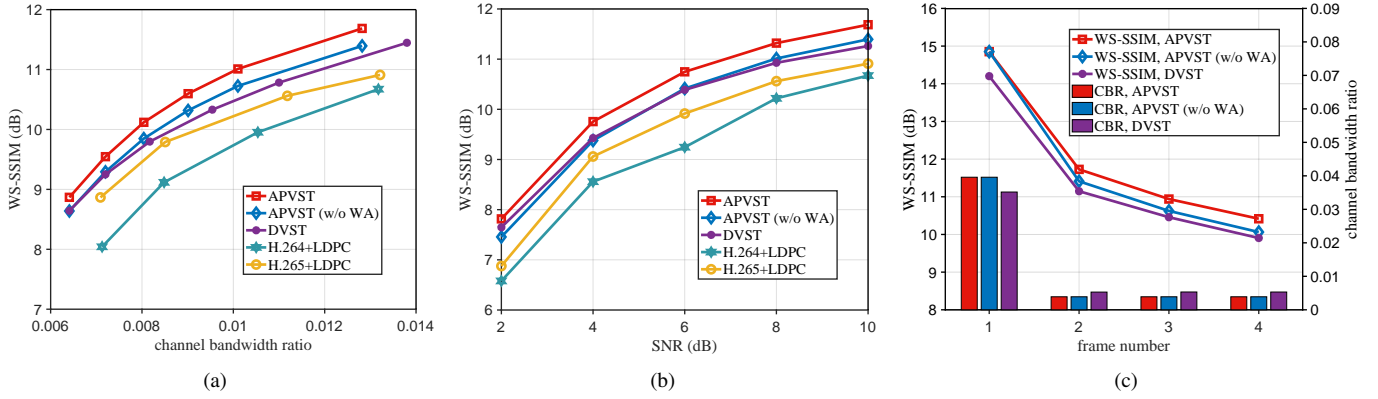


Fig. 5. (a) WS-SSIM performance versus channel bandwidth ratio (CBR), (b) WS-SSIM performance versus SNR, and (c) WS-SSIM and CBR in a GoP over the AWGN channel at SNR=10dB.

erence frame, the channel bandwidth ratio is higher compared to the next few frames. The continuous and lossy nature of panoramic video frame transmission leads to the WS-PSNR gradual decrease within a GoP. Compared with DVST and APVST (w/o WA) schemes, the proposed APVST achieves overall gains of about 2.4 dB and 1.1 dB in WS-PSNR under the condition of equal total CBR.

Fig. 5 shows WS-SSIM achieved by the five schemes varies with CBR and SNR. Similar to the trends observed with WS-PSNR, the proposed APVST scheme can save about 20% and 40% on channel bandwidth cost compared with DVST and H.264 + LDPC schemes. This further demonstrates that the APVST can provide a superior immersive experience in panoramic video transmission with less resource consumption.

V. CONCLUSION

In this paper, we propose the APVST network, which is based on the Deep JSCC structure and an attention mechanism, aimed at achieving semantic wireless adaptive end-to-end transmission of panoramic video. We propose a latitude adaptive module which is tailored to the specific characteristics of panoramic videos to save bandwidth. To pursue the higher WS-PSNR and WS-SSIM, a WA module is proposed, which works by fusing weights and semantic features. Experimental results demonstrate that the proposed APVST scheme outperforms other video transmission schemes. For future work, we will integrate the proposed APVST scheme with rate-splitting multiple access (RSMA) technology to further enhance the end-to-end transmission efficiency of panoramic videos.

REFERENCES

- [1] A. Yazar, S. Doğan-Tusha, and H. Arslan, "6G vision: an ultra-flexible perspective," *arXiv preprint, arXiv:2009.07597*, 2020.
- [2] Y. Sun, Z. Chen, M. Tao, and H. Liu, "Communications, caching, and computing for mobile virtual reality: modeling and tradeoff," *IEEE Trans. Commun.*, vol. 67, no. 11, pp. 7573-7586, Nov. 2019.
- [3] M. Zink, R. Sitaraman and K. Nahrstedt, "Scalable 360° video stream delivery: challenges, solutions, and opportunities," *Proc. IEEE*, vol. 107, no. 4, pp. 639-650, April 2019.
- [4] H. Xiao et al., "A transcoding-enabled 360° VR video caching and delivery framework for edge-enhanced next-generation wireless networks," *IEEE J. Sel. Areas Commun.*, vol. 40, no. 5, pp. 1615-1631, May 2022.
- [5] P. Zhang, W. Xu, H. Gao et al., "Toward wisdom-evolutionary and primitive-concise 6G: a new paradigm of semantic communication networks," *Engineering*, vol. 8, pp. 60-73, 2022.
- [6] Y. Li, X. Qin, K. Han, N. Ma, X. Xu and P. Zhang, "Accelerating wireless federated learning with adaptive scheduling over heterogeneous devices," *IEEE Internet Things J.*, vol. 11, no. 2, pp. 2286-2302, Jan. 2024.
- [7] E. Uysal et al., "Semantic communications in networked systems: a data significance perspective," *IEEE Netw.*, vol. 36, no. 4, pp. 233-240, August 2022.
- [8] Xu, X., Xiong, H., Wang, Y. et al., "Knowledge-enhanced semantic communication system with OFDM transmissions," *Sci. China Inf. Sci.*, vol. 66, no. 7, pp. 172302, 2023.
- [9] B. Xu, R. Meng, Y. Chen, X. Xu, C. Dong, and H. Sun, "Latent semantic diffusion-based channel adaptive De-Noising SemCom for future 6G systems," *arXiv preprint, arXiv:2304.09420*, 2023.
- [10] J. Li, B. Li, and Y. Lu, "Deep contextual video compression," *arXiv preprint, arXiv:2109.15047*, 2021.
- [11] S. Wang et al., "Wireless deep video semantic transmission," *IEEE J. Sel. Areas Commun.*, vol. 41, no. 1, pp. 214-229, Jan. 2023.
- [12] M. Li, J. Li, S. Gu, F. Wu, and D. Zhang, "End-to-end optimized 360° image compression," *IEEE Trans. Image Process.*, vol. 31, pp. 6267-6281, Sept. 2022.
- [13] Y. Sun, A. Lu, and L. Yu, "Weighted-to-spherically-uniform quality evaluation for omnidirectional video," *IEEE Signal Process. Lett.*, vol. 24, no. 9, pp. 1408-1412, Sept. 2017.
- [14] Y. Zhou, M. Yu, H. Ma, H. Shao and G. Jiang, "Weighted-to-spherically-uniform SSIM objective quality evaluation for panoramic video," *2018 14th IEEE International Conference on Signal Processing (ICSP)*, Beijing, China, pp. 54-57, 2018.
- [15] S. Woo, J. Park, J.-Y. Lee, and I. S. Kweon, "CBAM: convolutional block attention module," *arXiv preprint, arXiv:1807.06521*, 2018.
- [16] J. Ballé, V. Laparra, and E. P. Simoncelli, "End-to-end optimized image compression," *arXiv preprint, arXiv:1611.01704*, 2016.
- [17] E. Agustsson, D. Minnen, N. Johnston, J. Ballé, S. J. Hwang, and G. Toderici, "Scale-space flow for end-to-end optimized video compression," *IEEE Conf. Comput. Vis. Pattern Recognit.*, pp. 8500-8509, 2020.
- [18] Z. Liu et al., "Swin transformer v2: scaling up capacity and resolution," *arXiv preprint, arXiv:2111.09883*, 2021.
- [19] J. Ballé, V. Laparra, and E. P. Simoncelli, "Density modeling of images using a generalized normalization transformation," *arXiv preprint, arXiv:1511.06281*, 2015.
- [20] A. A. Baniya, T.-K. Lee, P. W. Eklund, and S. Aryal, "Omnidirectional video super-resolution using deep learning," *IEEE Trans. Multimedia*, pp. 1-15, Apr. 2023.
- [21] Y. Xu et al., "Gaze prediction in dynamic 360° immersive videos," *IEEE Conf. Comput. Vis. Pattern Recognit.*, pp. 5333-5342, 2018.
- [22] J. Dai et al., "Nonlinear transform source-channel coding for semantic communications," *IEEE J. Sel. Areas Commun.*, vol. 40, no. 8, pp. 2300-2316, Aug. 2022.
- [23] D. B. Kurka and D. Gündüz, "DeepJSCC-f: Deep joint source-channel coding of images with feedback," *IEEE J. Sel. Areas Inf. Theory*, vol. 1, no. 1, pp. 178-193, May 2020.